Simulation of transition from Townsend mode to glow discharge mode in a helium dielectric barrier discharge at atmospheric pressure*

Li Xue-Chen(李雪辰)†, Niu Dong-Ying(牛东莹), Xu Long-Fei(许龙飞), Jia Peng-Ying(贾鹏英), and Chang Yuan-Yuan(常媛媛)

College of Physics Science & Technology, Hebei University, Baoding 071002, *China*

(Received 28 November 2011; revised manuscript received 20 January 2012)

The dielectric barrier discharge characteristics in helium at atmospheric pressure are simulated based on a one-dimensional fluid model. Under some discharge conditions, the results show that one discharge pulse per half voltage cycle usually appears when the amplitude of external voltage is low, while a glow-like discharge occurs at high voltage. For the one discharge pulse per half voltage cycle, the maximum of electron density appears near the anode at the beginning of the discharge, which corresponds to a Townsend discharge mode. The maxima of the electron density and the intensity of electric field appear in the vicinity of the cathode when the discharge current increases to some extent, which indicates the formation of a cathode-fall region. Therefore, the discharge has a transition from the Townsend mode to the glow discharge mode during one discharge pulse, which is consistent with previous experimental results.

Keywords: dielectric barrier discharge, atmosphere pressure glow discharge, discharge mode, Townsend discharge

PACS: 52.80.Tn, 52.80.Hc, 52.80.Mg **DOI:** 10.1088/1674-1056/21/7/075204

1. Introduction

In recent years atmospheric pressure glow discharge (APGD) has received extensive attention. This kind of discharge has many industrial applications, such as surface modification,[1] ozone generation, biological sterilization,[2] and pollution control[3] due to its ability to dispense with expensive vacuum systems.[4]

The discharge mechanism has been investigated both experimentally and numerically. For numerical simulation, continuity equations coupled with Poisson's equation are usually solved to investigate the discharge mechanism. Since calculating the solution of the electric field from Poisson's equation is a complicated and time-consuming procedure, Kulikovsky[5] put forward a new way of using the current conservation equation instead of Poisson's equation. With this method, the characteristics of APGD controlled by a dielectric barrier with electrodes in several different geometries, such as parallel plate geometry, and coaxial geometry have been investigated.[6−9] Their results show that the homogeneous dielectric barrier discharge at atmospheric pressure in helium is usually featured by one current peak per half cycle of the applied voltage and the space structure of this discharge is similar to that of low pressure glow discharge. It has also been found that the discharge can operate in either Townsend mode or glow mode under different operational conditions.

In experimental studies, intensified charge couple device (ICCD) cameras are often used to take images of the discharge gap.[10] In Ref. [10], temporally resolved images are taken in one discharge pulse by an ICCD camera in helium at atmospheric pressure. Therefore, the spatiotemporal distribution of light emission intensity is obtained. A transition from a Townsend discharge to a glow one is observed experimentally during one discharge pulse. However, it has not been studied numerically. In this paper, the

*Project supported by the National Natural Science Foundation of China (Grant Nos. 10805013 and 51077035), the Funds for Distinguished Young Scientists of Hebei University, China (Grant No. A2012201045) the Key Project of Ministry of Education of China (Grant No. 210014), the Natural Science Foundation of Hebei province, China (Grant Nos. A2009000149 and A2011201132), and the Outstanding Youth Project of Education Department of China (Grant No. Y2011120).

†Corresponding author. E-mail: xcli@mail.hbu.edu.cn

transition is investigated numerically based on a one-dimensional fluid model.

2. Simulation model

The discharge is generated between two parallel–plate electrodes covered by dielectric layers, as shown in Fig. 1. A sinusoidal voltage $V_{\rm a}(t) = U_{\rm p}\sin(2\pi ft)$ is applied between the two electrodes. The thicknesses of two dielectric layers are d_1 and d_2, respectively. The discharge gap is $d_{\rm g}$ and d is the distance between the metallic electrodes.

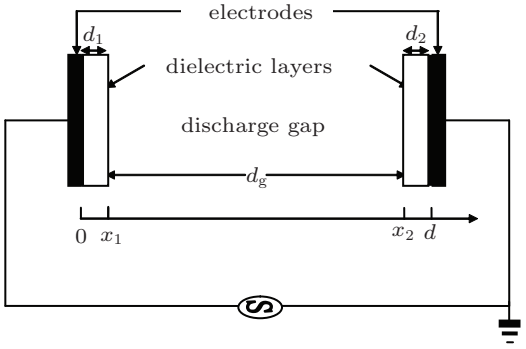

Fig. 1. Electrode configuration used in the present model.

Pure helium is used as the working gas. The numerical simulation is based on a one-dimensional fluid model. Electrons and ions are described by the continuity equations as follows:

$$\frac{\partial n_{\rm e,p}}{\partial t} + \frac{\partial j_{\rm e,p}}{\partial x} = S, \tag{1}$$

where n is the particle density, j is the flux, S is the source term, and subscripts e and p represent the electrons and ions, respectively. In the source term, the direct ionization by electron impact and electron–ion recombination are considered.

$$S = \alpha\mu_{\rm e}\,|E|\,n_{\rm e} - \beta n_{\rm e}n_{\rm p}, \tag{2}$$

where α, β, and $\mu_{\rm e}$ are Townsend ionization coefficients, electron-ion recombination rate coefficients, and electron mobility, whose values are identical to those used in Refs. [11]–[13]. Furthermore, $j_{\rm e,p}$ can be obtained from the momentum equation as

$$j_{\rm e,p} = \mp\mu_{\rm e,p}n_{\rm e,p}E - D_{\rm e,p}\frac{\partial n_{\rm e,p}}{\partial x}, \tag{3}$$

where μ and D are the mobility and diffusion coefficients, whose values are taken from Ref. [12].

Instead of Poisson's equation, the electric field is obtained from the current conservation equation[5]

$$\varepsilon(x)\frac{\partial E(x,t)}{\partial t} + i_{\rm C}(x,t) = i_{\rm T}(t), \tag{4}$$

where $i_{\rm T}$ is the total current density, $i_{\rm C}$ is the conduction current density, and $\varepsilon(x)$ is the permittivity and depends on the position. $\varepsilon(x) = \varepsilon_0$ in the gas region and $\varepsilon(x) = \varepsilon_0\varepsilon_{\rm b}$ in the dielectric layers, where $\varepsilon_{\rm b}$ is the relative permittivity of the dielectric barrier. The electric field satisfies the following condition:

$$\int_0^d E(x,t)\,{\rm d}x = V_{\rm a}(t). \tag{5}$$

The conduction current density $i_{\rm C}$ is determined in terms of $j_{\rm p}$ and $j_{\rm e}$ as

$$i_{\rm C}(x,t) = e(j_{\rm p}(x,t) - j_{\rm e}(x,t)), \tag{6}$$

where $j_{\rm p}$ and $j_{\rm e}$ are respectively the ion and electron fluxes, which are derived from Eq. (3). Secondary electron emissions from the instantaneous cathode are considered here for ion bombardment alone, and therefore the electron flux leaving the cathode is taken as $\gamma j_{\rm p}(x,t)$. Here γ is the secondary emission coefficient. The expression of $i_{\rm T}$ can be obtained by integrating Eq. (4) from $x = 0$ to $x = d$ as

$$i_{\rm T}(t) = \left(d_{\rm g} + \frac{d_1+d_2}{\varepsilon_0}\right)^{-1} \times \left[\int_{x_1}^{x_2} i_{\rm C}(x,t)\,{\rm d}x - \varepsilon_0\frac{\partial V_{\rm a}(t)}{\partial t}\right]. \tag{7}$$

3. Results and discussion

In our simulation the above set of equations is solved by the semi-implicit Scharfetter–Gummel scheme.[14,15] The simulation parameters are chosen as follows. The discharge gap $d_{\rm g}$ is fixed to be 2.0 mm, the gas pressure is about 1.01×10^5 Pa, the gas temperature is 300 K, and the electron energy is 1.5 eV. The secondary electron emission coefficient γ is assumed to be 0.01, and the thicknesses of the dielectric layers are the same ($d_1 = d_2 = 1.0$ mm) with their relative permittivity $\varepsilon_{\rm b}$ being 7.5. The initial electron and ion densities in the gas gap are considered to be uniform, i.e., $n_{\rm e}(x,0) = n_{\rm p}(x,0) = 10^7$ cm^{-3}. Since the initial value of surface charge density has no effect on the discharge characteristics after the discharge has reached a steady state (about 20 discharge cycles), it can be chosen arbitrarily. In this paper, the initial value is

chosen to be zero. Unless otherwise stated, the amplitude (U_p) and driving frequency (f) of the applied sinusoidal voltage are 1.5 kV and 33 kHz, respectively.

Figure 2 shows the waveform of the applied voltage V_a, gas voltage V_g, and total current i_T under different values of U_p. From Fig. 2(a), it can be found that there is only one discharge current pulse per half cycle of the applied voltage when U_p is low (1500 V), which is an indication of APGD.[16] Figure 2(b) shows the scenario at $U_p = 1700$ V. Apart from the increasing amplitude of i_T, the waveform of i_T is similar in shape to that shown in Fig. 2(a). When the value of U_p increases to 2300 V, two current pulses appear per half cycle of the applied voltage, as shown in Fig. 2(c). Figure 2(d) illustrates that more current peaks are formed when U_p is 3000 V. The discharge modes shown in Figs. 2(c) and 2(d) are both glow-like discharges as indicated in Ref. [17]. Consequently, it can be concluded that the discharge mode changes from APGD to a glow-like discharge with U_p increasing.

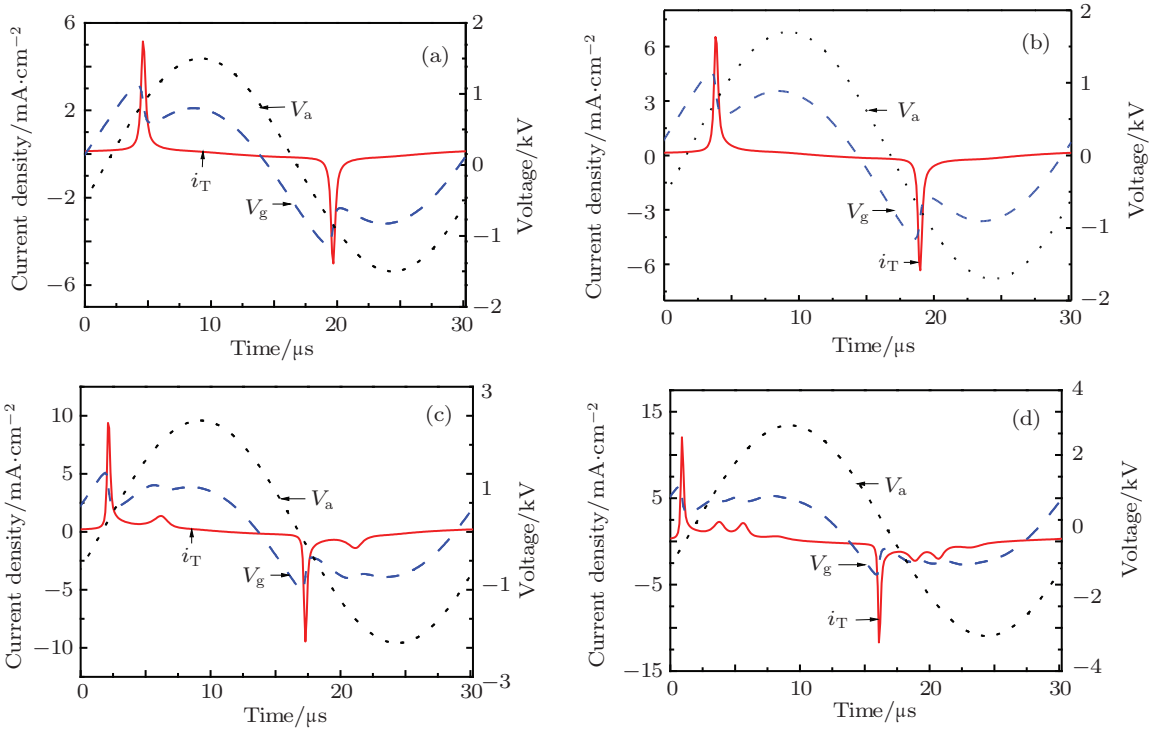

Fig. 2. (colour online) Waveforms of applied voltage (V_a), gas voltage (V_g) and total current (i_T) at (a) $U_p = 1500$ V, (b) 1700 V, (c) 2300 V, and (d) 3000 V.

Figure 3(a) indicates the inception value of the applied voltage (V_{ain}) as a function of U_p. It can be found that V_{ain} decreases with the increase of U_p. When V_{ain} is less than zero, it is called the discharge before zero-voltage. This phenomenon of discharge before zero-voltage has been found experimentally by Dong *et al.*[18] They attributed it to the effect of wall charges on the dielectric. As shown in Fig. 2, the discharge is the APGD mode for one discharge pulse per half cycle. Figures 3(b) and 3(c) show the peak value of i_T as a function of U_p and f under this APGD mode, respectively. It can be found that i_T changes almost linearly with U_p and f. In order to explain the linear relationship, an equivalent circuit of the discharge in parallel plate geometry is given in Fig. 4. From the equivalent circuit, the total current i_T can be deduced as follows:[19]

$$i_T \approx 2\pi f U_p C_b. \tag{8}$$

Here, C_b is the capacitance of the dielectric layer. Formula (8) shows that i_T is proportional to U_p as well as f. That is to say, i_T changes linearly with U_p with constant f, which is consistent with the result shown in Fig. 3(b). Furthermore, i_T is proportional to f with constant U_p, which is consistent with the result shown in Fig. 3(c).

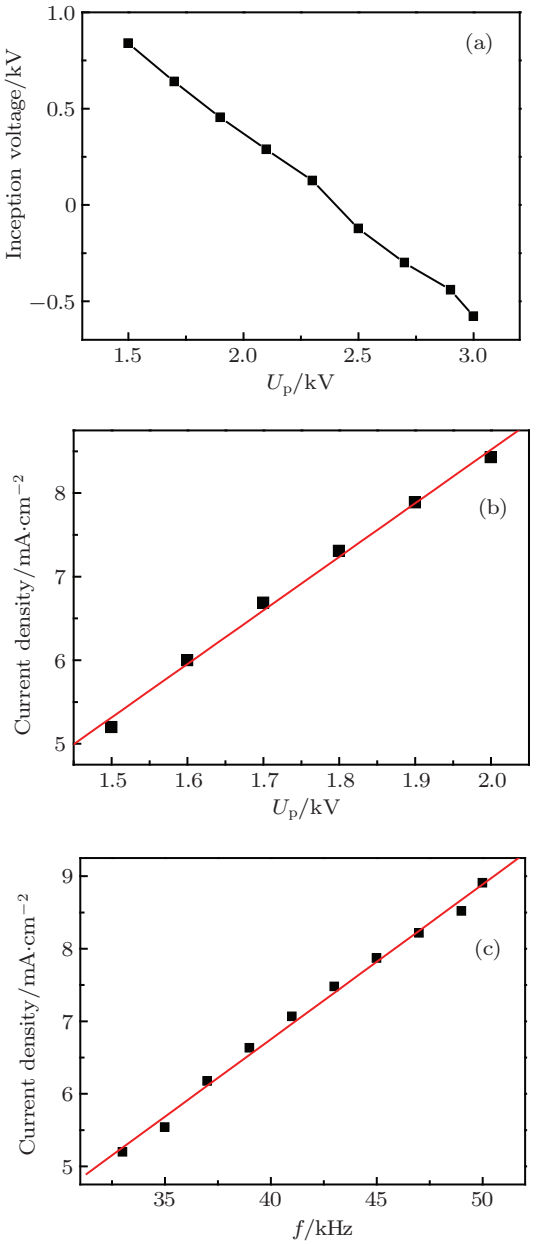

Fig. 3. (colour online) (a) The inception voltage as a function of U_p. (b) The peak value of i_T as a function of U_p at a driving frequency of 33 kHz. (c) The peak value of i_T as a function of f with U_p being 1.5 kV.

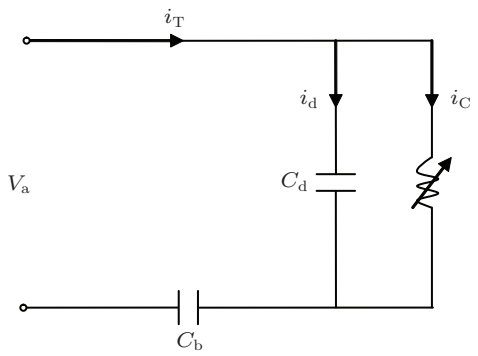

Fig. 4. An equivalent circuit of the discharge in parallel plate geometry.

Figure 5 shows an enlarged part of the discharge current i_T corresponding to the scenario shown in Fig. 2(a). Points A to G correspond to the moments at 1.0, 3.7, 3.9, 4.1, 4.3, 4.5, and 4.6 μs, respectively.

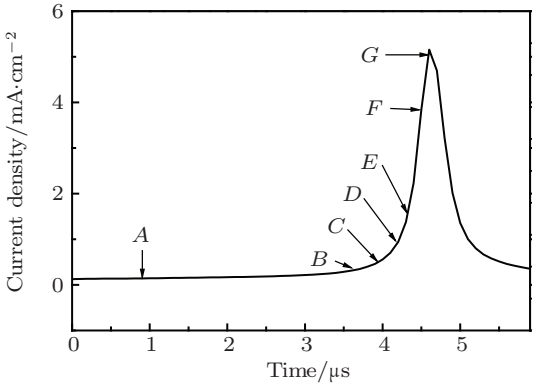

Fig. 5. An enlarged part of the discharge current i_T corresponding to that shown in Fig. 2(a).

Figure 6 shows the spatial distributions of electron density, ion density, and the electric field corresponding to the moments A to G, respectively. At the very beginning of the discharge (moment B), the maximum of electron density appears at the anode. The electric field as well as the ion density are almost uniformly distributed along the gap. Such a behaviour is a typical Townsend breakdown mechanism. In Townsend mode, electron avalanches develop from the cathode to the anode. The number of electrons increases in the process. Therefore, the maximum electron density appears at the anode. It can also be found from Fig. 6 that the maximum of electron density shifts toward the cathode with the discharge moment changing, the number of ions near the cathode rapidly increases, and the electric field also increases in front of the cathode. At moment G, a cathode-fall region can be discerned in Fig. 6(c), which implies that the discharge mode has been converted into a glow discharge mode. Therefore, it can be concluded that the discharge mode transits from a Townsend discharge to a glow discharge during one current pulse for APGD.

As is well known, the intensity of the light emission is proportional to the density of excited atoms. Furthermore, the excited atom density is determined by the electron density. Therefore, figure 6(a) also indicates that the maximum of the light emission appears at the anode at the beginning of the discharge pulse. With time passing by, the maximum of the light emission shifts towards the cathode. At moment G, the maximum of light emission intensity appears near the cathode after the cathode-fall region is formed.

These phenomena are consistent with the experimental results reported in Ref. [10].

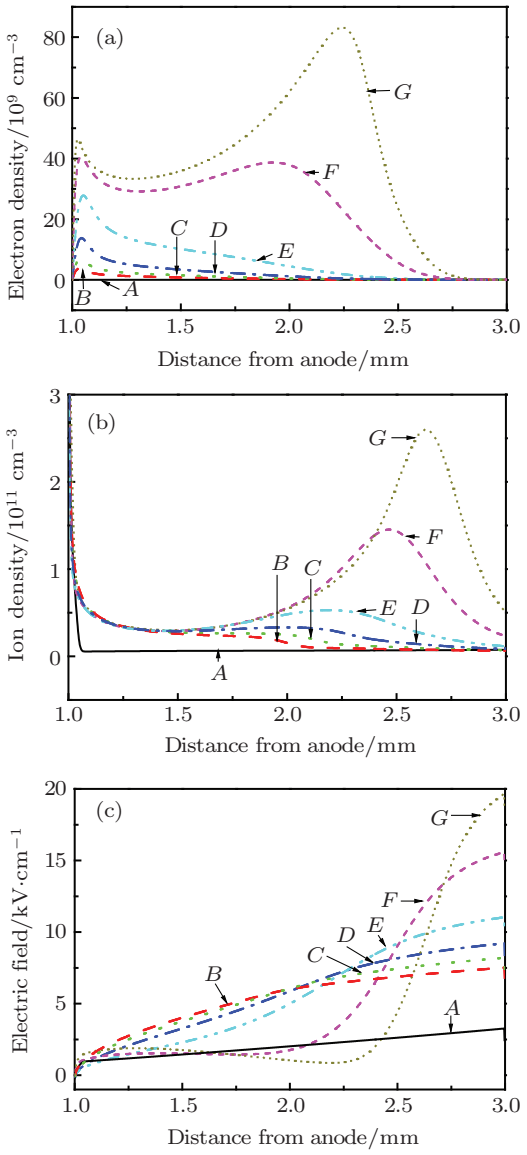

Fig. 6. (colour online) Spatial distributions of (a) electron density, (b) ion density, and (c) electric field at different moments. Points *A*–*G* correspond to those shown in Fig. 5.

4. Conclusion

Based on a one-dimensional fluid model, dielectric barrier discharge characteristics in helium at atmospheric pressure are numerically investigated. The results show that the discharge mode changes from APGD to a glow-like discharge with $U_{\rm p}$ increasing. The phenomenon of discharge before zero-voltage is found when $U_{\rm p}$ increases to a certain value. It has also been found that $i_{\rm T}$ changes linearly with $U_{\rm p}$ and driving frequency. For APGD, at the very beginning of discharge, the maxima of electron density and light emission intensity appear at the anode, which corresponds to a Townsend discharge mode. A cathode-fall region can be discerned and the maximum of light emission appears in the vicinity of the cathode with the discharge moment changing, which implies that the discharge mode is converted into a glow discharge mode. Therefore, it can be concluded that the discharge has a transition from Townsend mode to glow discharge mode during one discharge pulse. These numerical results are consistent with the experimental phenomena.

References

[1] Michael A. Lieberman 2005 *Principles of Plasma Discharges and Materials Processing* (published online) (New Jersey: John Wiley & Sons)

[2] Kim J Y, Kim S O, Wei Y Z and Li J H 2010 *Appl. Phys. Lett.* **96** 203701

[3] Ticos C M, Jepu I, Lungu C P, Chiru P, Zaroschi V and Lungu A M 2010 *Appl. Phys. Lett.* **97** 011501

[4] Li X C, Jia P Y, Yuan N, Fang T Z and Wang L 2011 *Phys. Plasmas* **18** 043505

[5] Kulikovsky A A 1994 *J. Phys.* D **27** 2556

[6] Wang Y H and Wang D Z 2004 *Chin. Phys. Lett.* **21** 2234

[7] Shi H, Wang Y H and Wang D Z 2008 *Phys. Plasmas* **15** 122306

[8] Liu F C, Zhang D Z and Wang D Z 2010 *Phys. Plasma* **17** 103508

[9] Zhang H Y, Wang D Z and Wang X G 2007 *Chin. Phys.* **16** 1089

[10] Luo H Y, Liang Z, Lü B, Wang X X, Guan Z C and Wang L M 2007 *Appl. Phys. Lett.* **91** 221504

[11] Ward A L 1962 *J. Appl. Phys.* **33** 2789

[12] Deloche R, Monchicourt P, Cheret M and Lambert F 1976 *Phys. Rev.* A **13** 1140

[13] Xu X J 1996 *Discharge Physics of Gas* (Shanghai: Fu-dan University Press) p. 277 (in Chinese)

[14] Scharferter D L and Gummel H K 1969 *IEEE Trans. Electron. Devices* **ED-16** 64

[15] Kulikovsky A A 1995 *J. Comput. Phys.* **119** 149

[16] Li X C, Zhao N, Fang T Z, Liu Z H, Li L C and Dong L F 2008 *Plasma Source Sci. Technol.* **17** 015017

[17] Trunec D, Brablec A and Stastny F 1998 *Contrib Plasma Phys.* **38** 435

[18] Dong L F, Mao Z G and Ran J X 2005 *Chin. Phys.* **14** 1618

[19] Golubovsii Y B, Majorov V A, Behnke J and Behnke J F 2002 *J. Phys.* D **35** 751